

**NEW**

$B \rightarrow KK\pi$  amplitude analysis

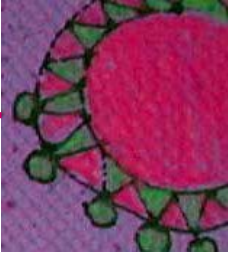
LHCb Preliminary

~~$B \rightarrow \pi\pi\pi$  amplitude analysis~~

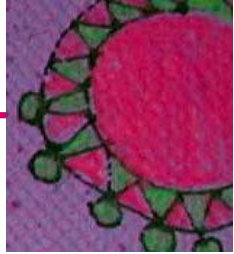
~~LHCb UnOfficial~~

Jussara Miranda ● CBPF-Rio de Janeiro ● for the LHCb collaboration





- overview
- $B \rightarrow KK\pi$  Amplitude analysis (AmAn)
  - data set
  - acceptance & background
  - model & fit
  - results
  - discussion
- $B \rightarrow \pi\pi\pi$  Amplitude analysis
- conclusions



- this is a followup (same dataset) on previous LHCb results:

PHYSICAL REVIEW D 90, 112004 (2014)

### Measurements of $CP$ violation in the three-body phase space of charmless $B^\pm$ decays

R. Aaij *et al.*\*

(LHCb Collaboration)

(Received 25 August 2014; published 11 December 2014)

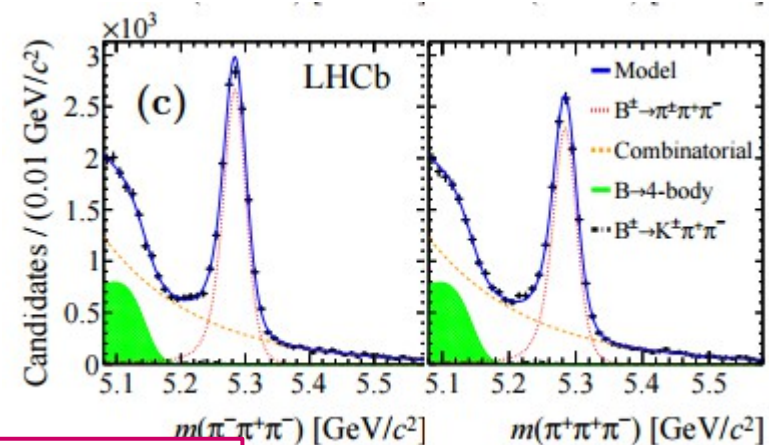
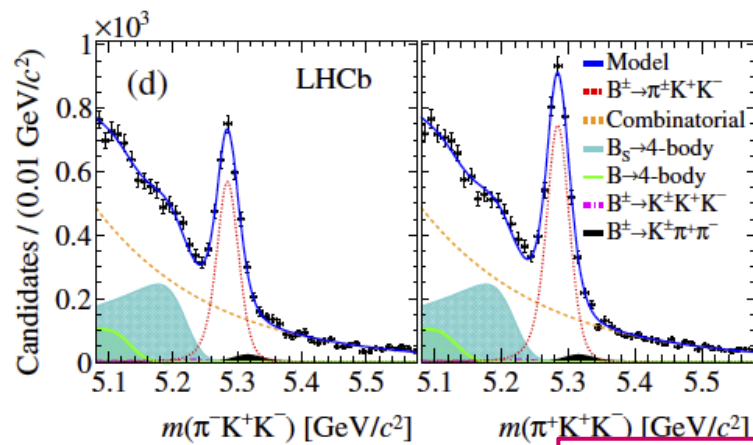
The charmless three-body decay modes  $B^\pm \rightarrow K^\pm \pi^+ \pi^-$ ,  $B^\pm \rightarrow K^\pm K^+ K^-$ ,  $B^\pm \rightarrow \pi^\pm K^+ K^-$  and  $B^\pm \rightarrow \pi^\pm \pi^+ \pi^-$  are reconstructed using data, corresponding to an integrated luminosity of  $3.0 \text{ fb}^{-1}$ , collected by the LHCb detector. The inclusive  $CP$  asymmetries of these modes are measured to be

$$A_{CP}(B^\pm \rightarrow K^\pm \pi^+ \pi^-) = +0.025 \pm 0.004 \pm 0.004 \pm 0.007,$$

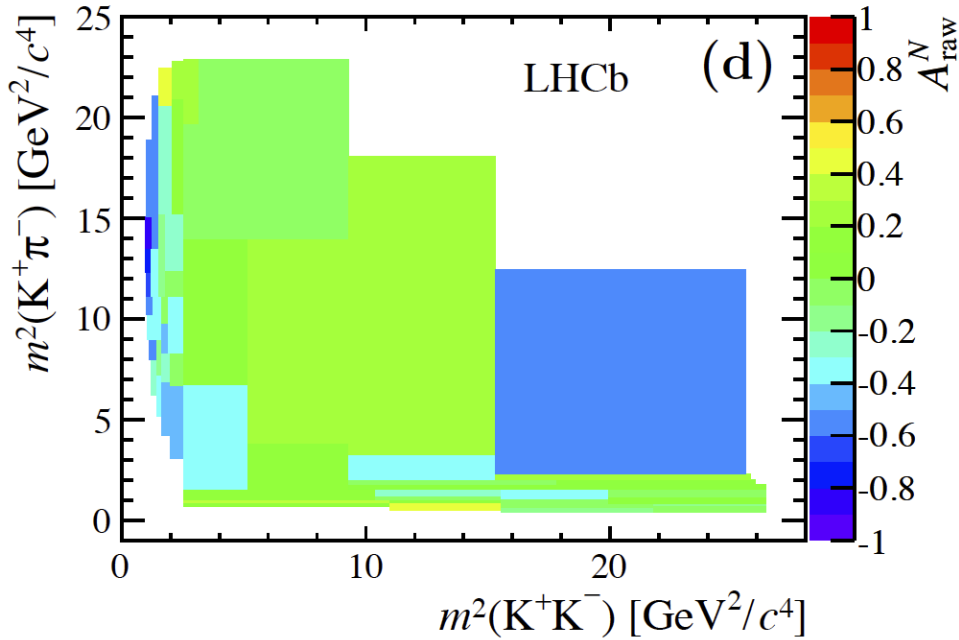
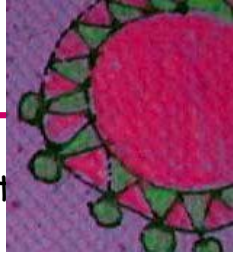
$$A_{CP}(B^\pm \rightarrow K^\pm K^+ K^-) = -0.036 \pm 0.004 \pm 0.002 \pm 0.007,$$

$$A_{CP}(B^\pm \rightarrow \pi^\pm \pi^+ \pi^-) = +0.058 \pm 0.008 \pm 0.009 \pm 0.007,$$

$$A_{CP}(B^\pm \rightarrow \pi^\pm K^+ K^-) = -0.123 \pm 0.017 \pm 0.012 \pm 0.007,$$

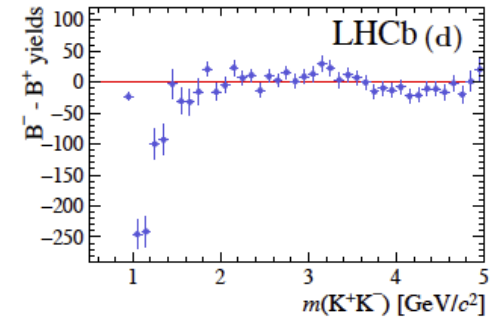
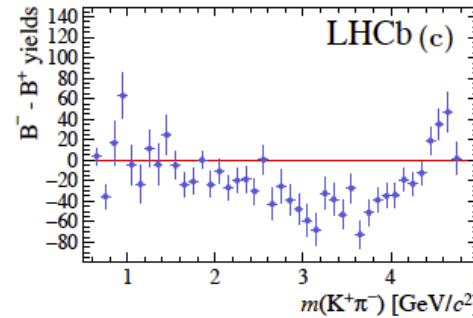
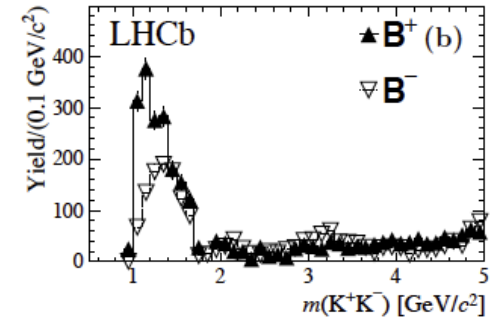
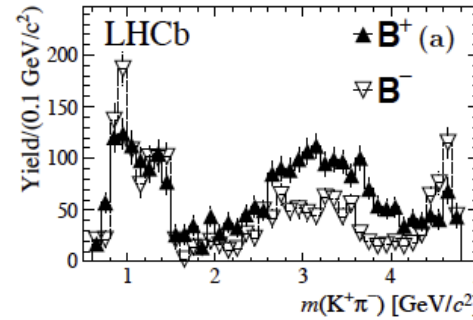


Decay mode	Yield
$B^\pm \rightarrow \pi^\pm \pi^+ \pi^-$	$24\,907 \pm 222$
$B^\pm \rightarrow \pi^\pm K^+ K^-$	$6\,161 \pm 172$

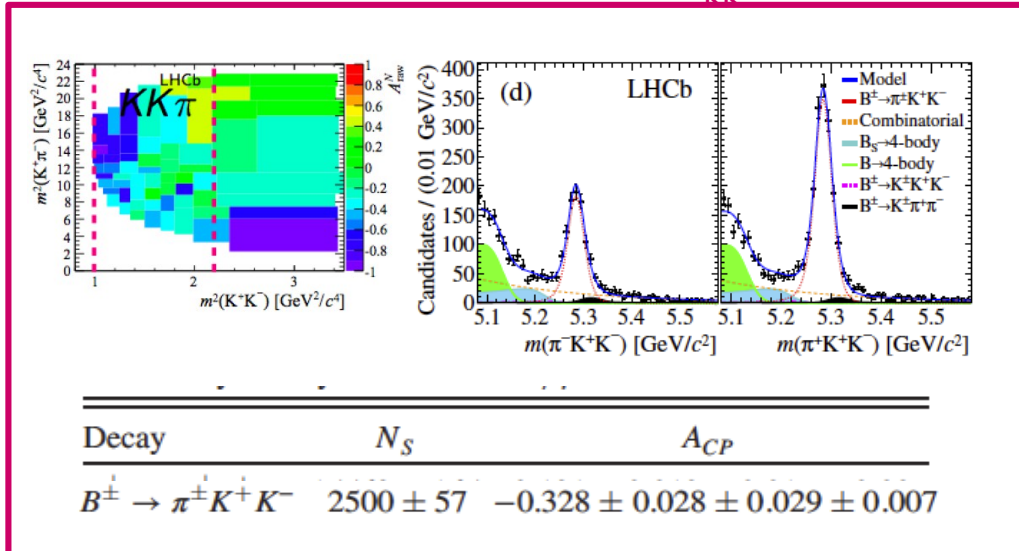


$$A_{\text{raw}}^N \equiv \frac{N^- - N^+}{N^- + N^+}$$

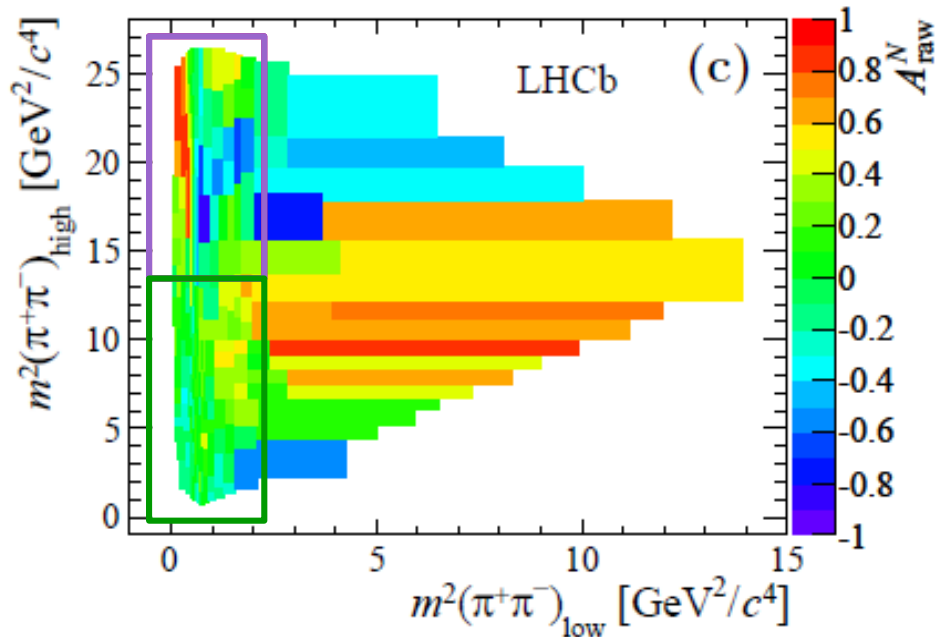
- N are acceptance corrected bkg subtracted yields
- Adaptive (B<sup>+</sup>+B<sup>-</sup>) binning



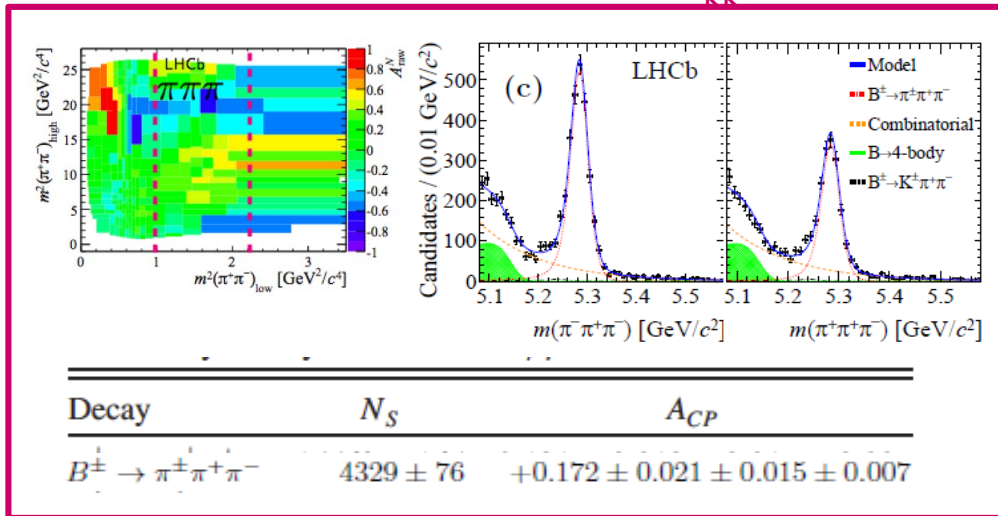
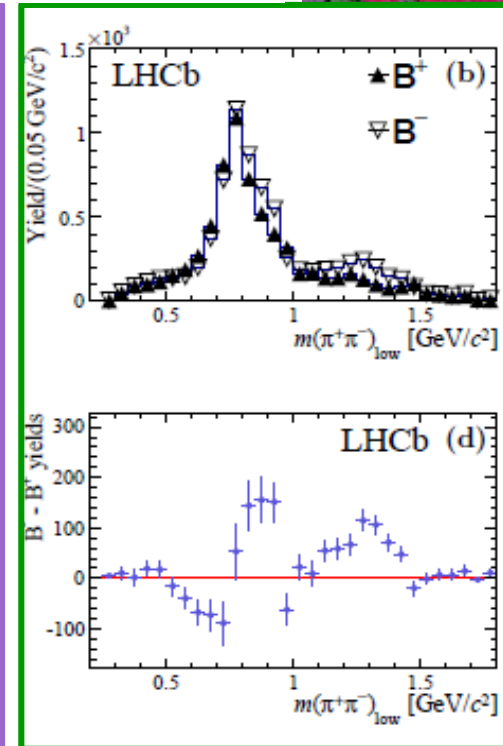
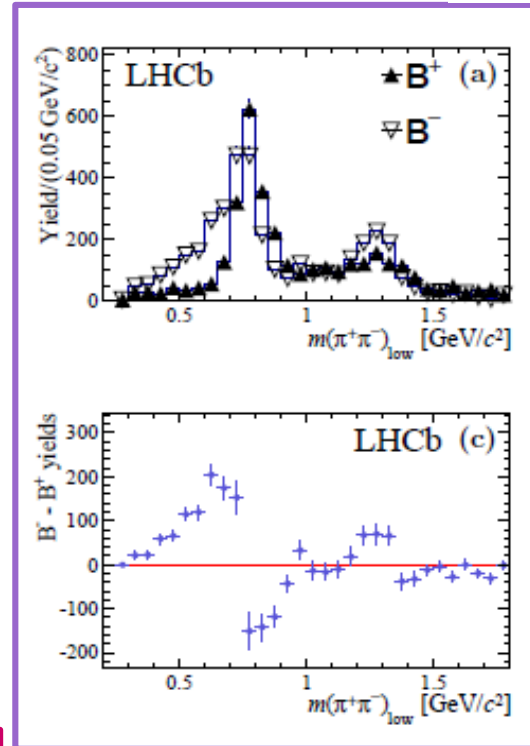
$m_{KK} < 1.5 \text{ GeV}$



Large CPV observed in the rescattering region ( $m_{KK}$  or  $m_{\pi\pi}$  between 1 and 1.5 GeV)

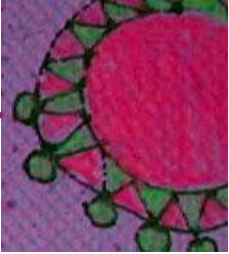


$m_{KK} < 1.5 \text{ GeV}$



rich interference pattern leading to positive and negative CPV discussed in J.R.A.Nogueira et al Phys. Rev. D92,054010 (2015)

large CPV observed in the rescattering region ( $m_{KK}$  or  $m_{\pi\pi}$  between 1 and 1.5 GeV)

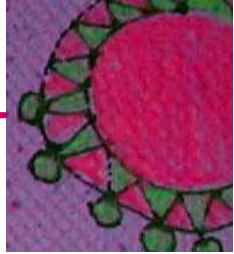


- large CPV observed in regions of the phase space :
  - some cancel out within the decay
  - some do not cancel ► CPV must be compensated to ensure CPT
- $B \rightarrow KK\pi$  and  $B \rightarrow \pi\pi\pi$  are connected by  $KK \leftrightarrow \pi\pi$  rescattering
- $KK \leftrightarrow \pi\pi$  rescattering is a way to ensure CPT
- hadronic effects play important role in CPV
- the CPV in phase space may be a manifestation of:
  - direct CPV on a intermediate state
  - interference of intermediate states with difference in strong and/or weak phases
  - $KK \leftrightarrow \pi\pi$  rescattering

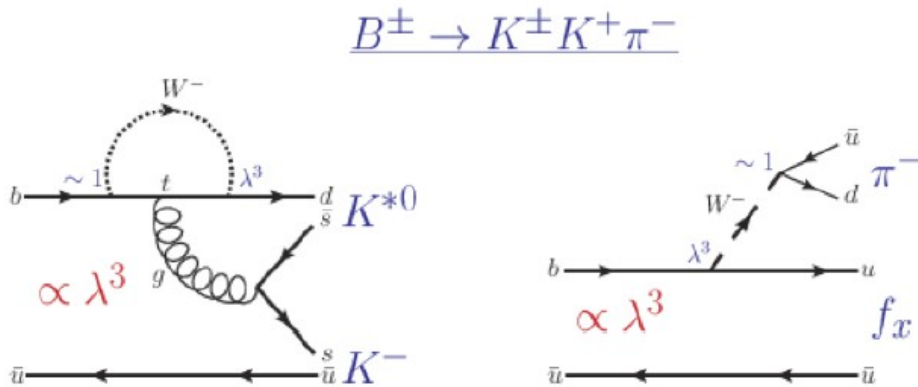
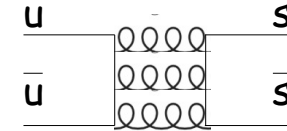
the amplitude analysis of the four channels will  
help elucidate and verify some hypotheses

# NEW $B \rightarrow KK\pi$ amplitude analysis

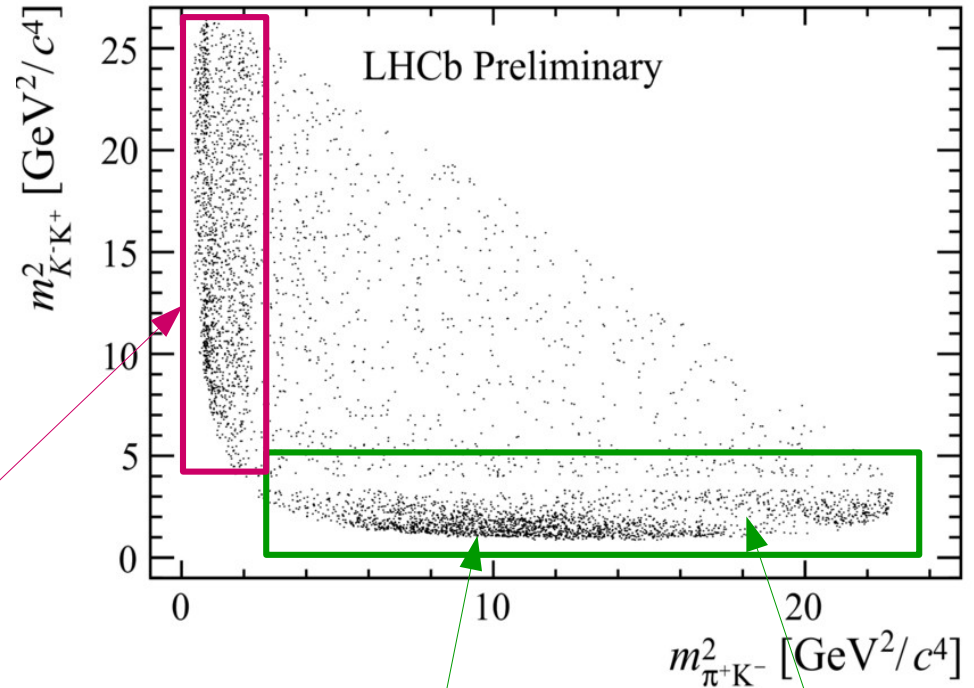
- **LHCb Preliminary**: approved by the review committee but yet under full collab. circulation
- first amplitude analysis ever performed for this channel



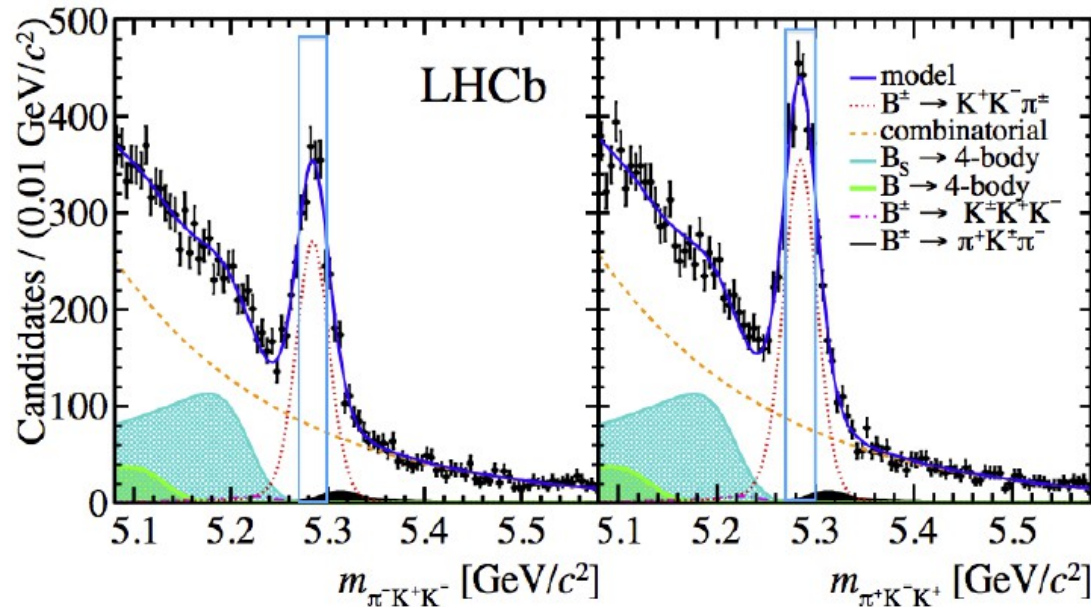
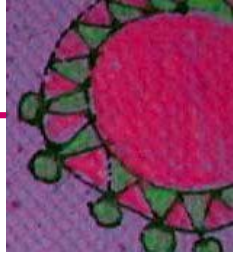
- simpler (in comparison to the other B → hhh channels) resonance structure,  $s\bar{s}$  states ( $\phi(1020)$  &  $f_0(980)$ ) are suppressed by OZI rule
- limited statistic



- Kπ: ●  $K^*(890)$ ,  $K^*(1430)$
- broad scalar

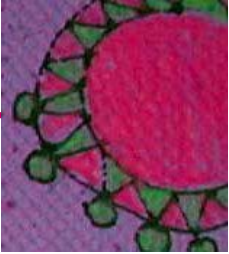


- KK: ● clear scalar low mass structure (CPV)
- interference pattern with higher spin resonance
- no  $\phi(1020)$



- 1D mass fit ► S/B in the signal region
- signal region : ●  $|5283 - m_B| < 17 \text{ MeV}$  ► narrow to avoid large systematic due to bkg modeling
  - Signal ~ 74%
  - Combinatorial Bkg ~ 23%
  - Peaking KTTT ~ 2.67%
  - 4-body ~ 0.25%                      negligible
  - KKK ~ 0.12%
- signal yields : B+ ►  $2052 \pm 102$                       B- ►  $1566 \pm 84$

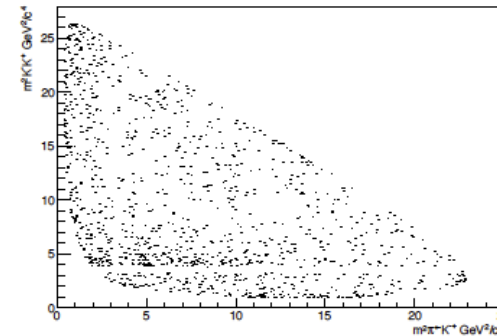
# $B \rightarrow KK\pi$ AmAn: acceptance backgrounds



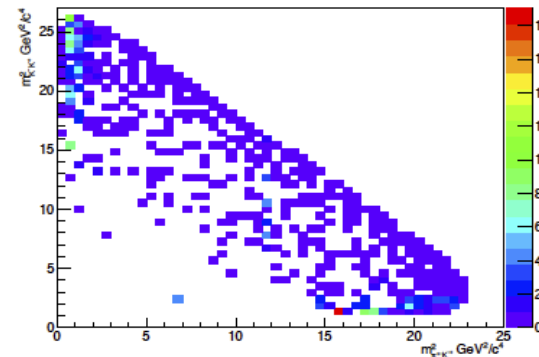
- **acceptance:** from Monte Carlo with correction for particle ID and hadronic trigger, taken from data, plus production and detection asymmetries.

- **backgrounds:**

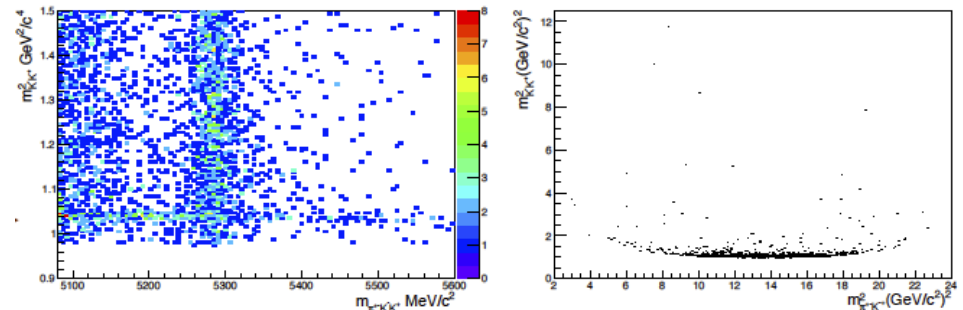
- **combinatorial background (~23%):**  
constructed using the right side events  
 $5400 < B_m < 5500 \text{ MeV}/c^2$

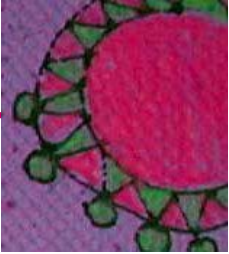


- **$K\pi\pi$  peaking background (~2.7%):**  
MC simulated  $B \rightarrow K\pi\pi$  mis-ID as  $B \rightarrow KK\pi$ , re-weighted to bring in the Dalitz plot structure based on BaBar model.



- **prompt produced  $\phi(1020)$  (+~0.6%):**  
use side bands to estimate the contamination in signal region and a ToyMC for  $\phi(1020) \rightarrow KK$  generated with no angular distribution





- **isobar model:** coherent sum of intermediate contributions

$$\mathcal{A}(m_{\pi^+K^-}^2, m_{K^-K^+}^2) = \sum_{i=1}^N c_i \mathcal{M}_{Ri}(m_{\pi^+K^-}^2, m_{K^-K^+}^2)$$

$$\overline{\mathcal{A}}(m_{\pi^-K^+}^2, m_{K^+K^-}^2) = \sum_{i=1}^N \overline{c}_i \overline{\mathcal{M}}_{Ri}(m_{\pi^-K^+}^2, m_{K^+K^-}^2)$$

- $c_i^\dagger$  complex coefficients extracted from fit to B+ and B- data

$$c_i = a_i^+ e^{i\delta_i^+} \quad \overline{c}_i = a_i^- e^{i\delta_i^-}$$

- direct CPV in i

$$A_{cp,i} = \frac{|\overline{c}_i|^2 - |c_i|^2}{|\overline{c}_i|^2 + |c_i|^2}$$

large CPV manifestation can come from difference in phases. **do not overlook**

- fit fraction

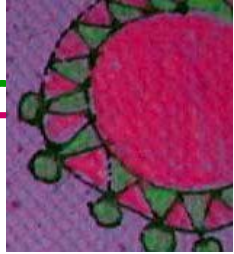
$$FF_i = \frac{\iint (|c_i \mathcal{M}_i|^2 + |\overline{c}_i \overline{\mathcal{M}}_i|^2) dm_{\pi^\pm K^\mp}^2 dm_{K^+K^-}^2}{\iint (|\mathcal{A}|^2 + |\overline{\mathcal{A}}|^2) dm_{\pi^\pm K^\mp}^2 dm_{K^+K^-}^2}$$

- use the fitting package LAURA++

**PRO:** freedom to "design" contributions  
ability to interpret the results

**CON:** require a robust model, difficult  
when involving broad scalar states,  
**over simplification**

# B → KKπ AmAn: model & fit



- $\mathcal{M}_{Ri}$  use quasi-two body approximation B → (hh)h not an imposition of isobar approach

- resonances: mostly<sup>†</sup> relativistic Breit-Wigner lineshapes with angular modulation and Blatt-Weisskopf barrier factors

$$\mathcal{M}_{Ri}(m_{\pi^+K^-}^2, m_{K^-K^+}^2) = P_i(J, \vec{p}, \vec{q}) F^B(|\vec{p}|) F^R(|\vec{q}|) T_{Ri}$$

Resonance Spin	Angular distribution
0	1
1	$-2\vec{p} \cdot \vec{q}$
2	$\frac{4}{3} [3(\vec{p} \cdot \vec{q})^2 - ( \vec{p}  \vec{q} )^2]$

Spin value $J$	Barrier Factors ( $F(z)$ )
$J = 0$	1
$J = 1$	$\sqrt{\frac{1+z_0^2}{1+z^2}}$
$J = 2$	$\sqrt{\frac{(z_0^4+3z_0^2+9)}{z^4+3z^2+9}}$

$$T_R(m_{ij}) = \frac{1}{m_R^2 - m_{ij}^2 - im_R\Gamma_{ij}(m_{ij})}$$

$$\Gamma_{ij}(m_{ij}) = \Gamma_R \left( \frac{|\vec{q}|}{|\vec{q}_R|} \right)^{2J+1} \frac{m_R}{m_{ij}} (F^2(|\vec{q}|d))$$

- SinglePoleFormFactor non-resonant: replaces the empirical exponential forms used in several occasions

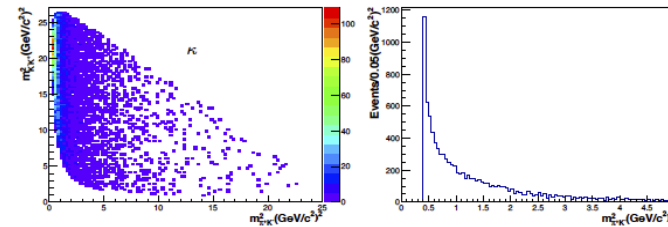
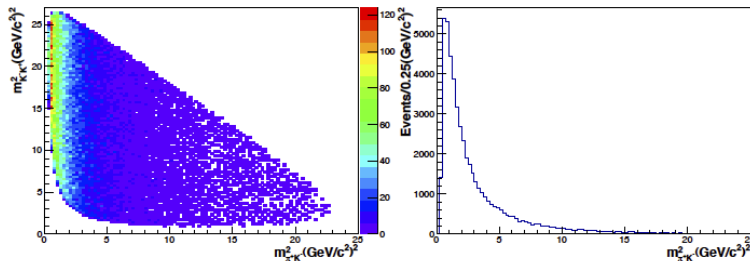
J.R.A.Nogueira et al, Phys.Rev. D92,0554010(2015)

$$T_{nr}(m_{ij}^2) = \frac{1}{1 + \frac{m_{ij}^2}{\Lambda^2}}$$

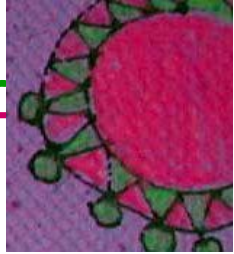
$\Lambda$  is a parameter that could be free in the fit.

Here  $\Lambda=1\text{GeV}/c^2$ , taken from B → πππ

- in our final fit this will replace the  $\kappa$  resonance



# B → KKπ AmAn: model & fit



- KK ↔ ππ rescattering: J.R.A.Nogueira et al Phys. Rev. D92,054010 (2015)

$$A_{scatt} = A_{source} f_{rescattering}$$

$$A_{source}(m_{K^-K^+}^2) = \frac{1}{1 + \frac{m_{K^-K^+}^2}{\Delta_{\pi\pi}^2}}$$

$$S = \begin{bmatrix} \eta e^{2i\delta_{\pi\pi}} & i\sqrt{1-\eta^2}e^{i(\delta_{\pi\pi}+\delta_{KK})} \\ i\sqrt{1-\eta^2}e^{i(\delta_{\pi\pi}+\delta_{KK})} & \eta e^{2i\delta_{KK}} \end{bmatrix}$$

- assuming  $\delta_{KK} = \delta_{\pi\pi}$

Pelaez & Yndurain PhysRevD71,074016(2005)

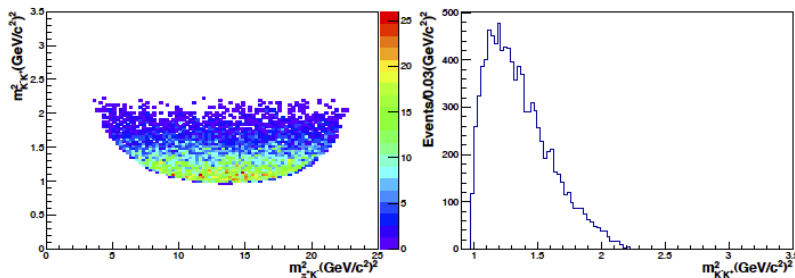
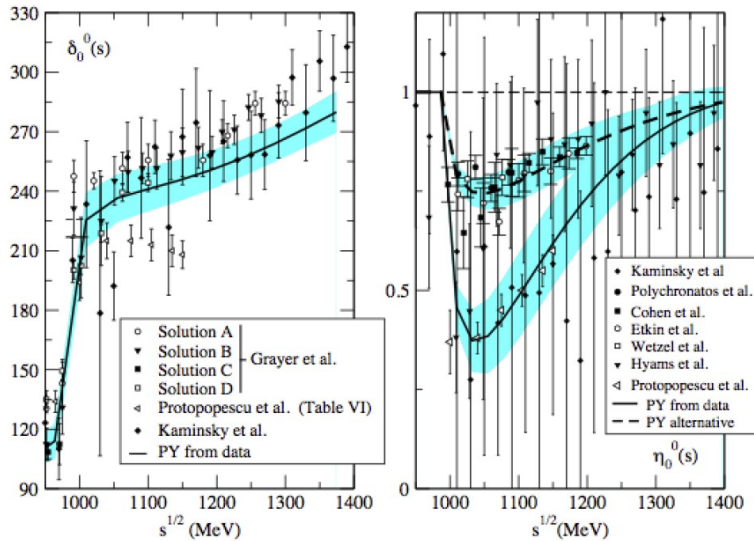
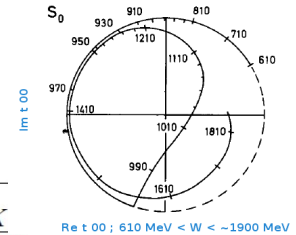
- fitting only ππ ↔ ππ (cern-Munich data) up to 1.4 GeV

$$\cot \delta_0^{(0)}(s) = c_0 \frac{(s - M_s^2)(M_f^2 - s)}{M_f^2 s^{1/2}} \frac{|k_2|}{k_2^2}, \quad k_2 = \frac{\sqrt{s - 4m_K^2}}{2},$$

$$\eta_0^{(0)} = 1 - \left( \epsilon_1 \frac{k_2}{s^{1/2}} + \epsilon_2 \frac{k_2^2}{s} \right) \frac{M'^2 - s}{s}.$$

$$c_0 = 1.3 \pm 0.5, \quad M_f = 1.320 \pm 50 \text{ GeV}; \quad M_s = 0.920 \text{ GeV (fixed)}$$

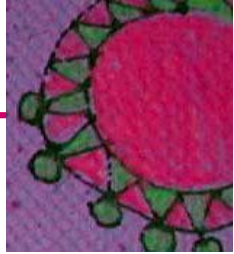
$$\epsilon_1 = 2.4, \quad \epsilon_2 = -5.5; \quad M' = 1.5 \text{ GeV (fixed)}.$$



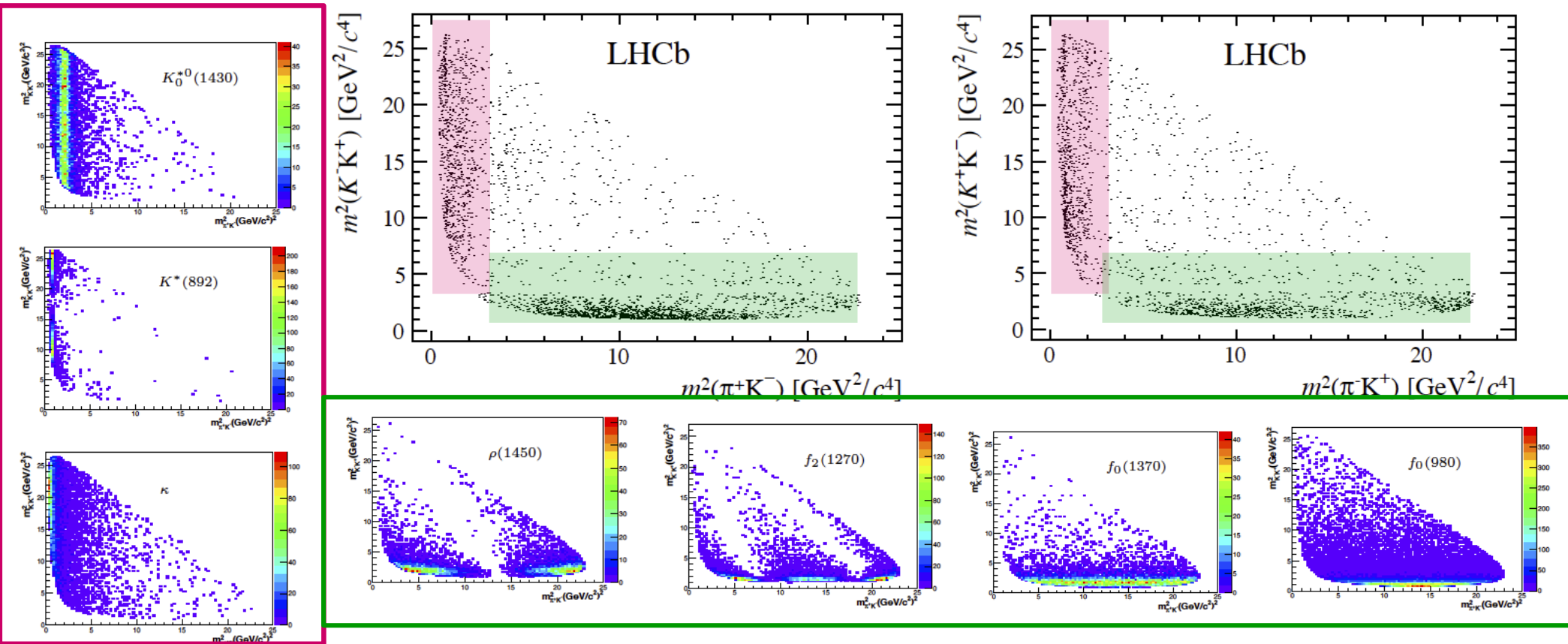
other parametrizations were tested

(including fitting parameters and Phys. Rev D 83 (2011) 074004)

there is room for improvement

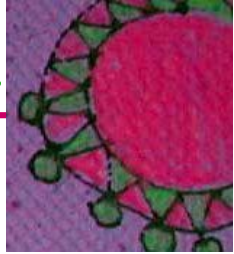


- **Fit strategy:** Start with well established resonances with relativistic Breit-Wigner or Flateé lineshapes and standard angular distribution and Baltt-Weisskopf barrier factors.
- of the many tested, 7 intermediate states are required to **reasonably** represent the data



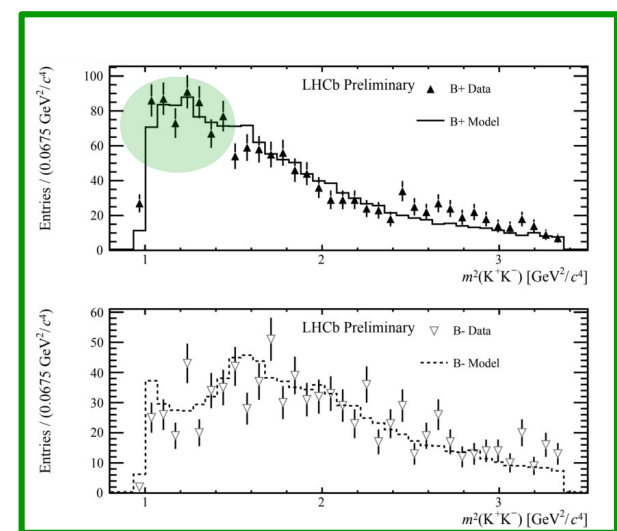
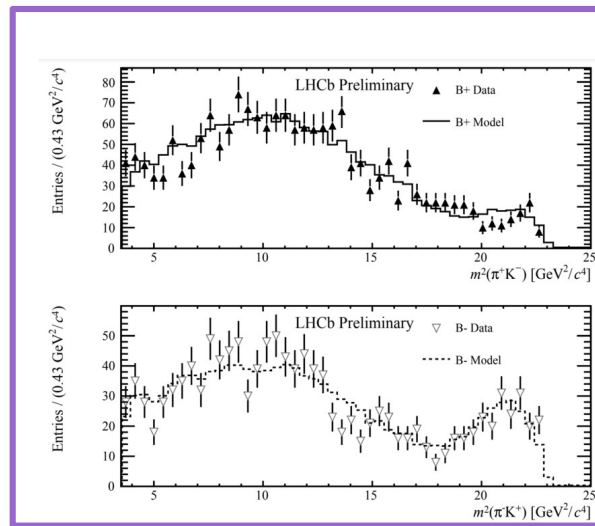
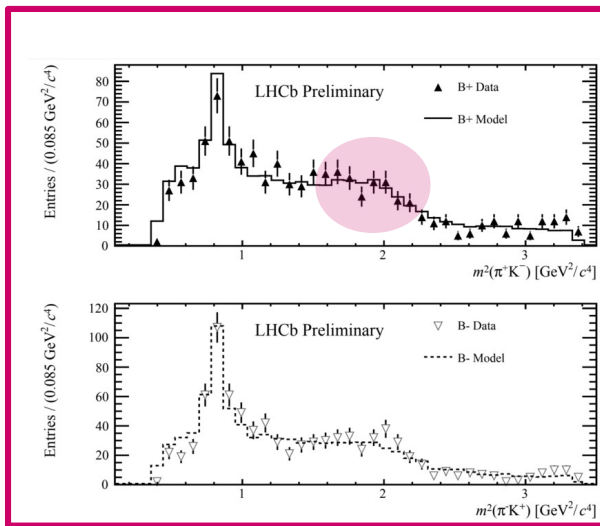
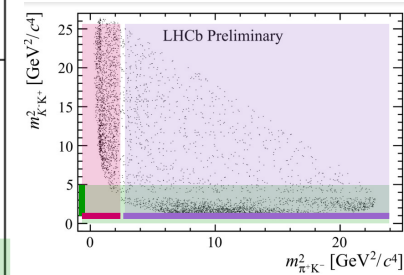
- **KK** in this model the large CPV is taken over by a large contribution of the  $f_0(980)$  that should be suppressed
- the very clear interference signature in high  $K\pi$  mass is solved by a scalar and a vector compatible with  $\rho(1450)$ , the tensor,  $f_2(1270)$  improves the fit.
- **Kπ** reasonably well represented by three components but can be improved

# B → KKπ AmAn: model & fit



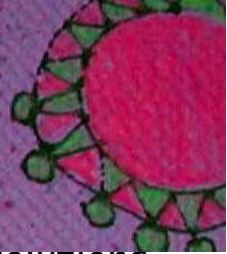
- final model:
  - $\kappa$  ▶ Single-Pole Form Factor
  - $f_0(980)$  &  $f_0(1370)$  ▶ rescattering
  - $\phi(1020)$

[NLL -9574] Component	Fit fraction (%)		Magnitude and phase coefficients				$A_{CP}$ (%)
	$B^+$	$B^-$	$a_i^+$	$\delta_i^+ [^\circ]$	$a_i^-$	$\delta_i^- [^\circ]$	
$K^{*0}(892)$	$5.7 \pm 0.8$	$9.9 \pm 1.0$	$0.94 \pm 0.04$	$0 \pm 0$	$1.06 \pm 0.04$	$0 \pm 0$	$12.3 \pm 8.7$
$K_0^{*0}(1430)$	$3.5 \pm 0.8$	$5.9 \pm 1.2$	$0.74 \pm 0.09$	$-176 \pm 10$	$0.82 \pm 0.09$	$136 \pm 11$	$10.4 \pm 14.9$
Single-Pole Form Factor	$31.0 \pm 2.0$	$34.1 \pm 2.6$	$2.19 \pm 0.13$	$-138 \pm 7$	$1.97 \pm 0.12$	$166 \pm 6$	$-10.7 \pm 5.3$
$\rho^0(1450)$	$29.5 \pm 1.5$	$32.4 \pm 1.9$	$2.14 \pm 0.11$	$-175 \pm 10$	$1.92 \pm 0.10$	$140 \pm 13$	$-10.9 \pm 4.4$
$f_2(1270)$	$4.7 \pm 0.9$	$11.2 \pm 1.3$	$0.86 \pm 0.09$	$-106 \pm 11$	$1.13 \pm 0.08$	$-128 \pm 11$	$26.7 \pm 10.2$
Rescattering	$23.7 \pm 1.1$	$6.5 \pm 0.8$	$1.91 \pm 0.09$	$-56 \pm 12$	$0.86 \pm 0.07$	$-81 \pm 14$	$-66.4 \pm 3.8$
$\phi(1020)$	$0.2 \pm 0.2$	$0.4 \pm 0.2$	$0.20 \pm 0.07$	$-52 \pm 23$	$0.22 \pm 0.06$	$107 \pm 33$	$9.8 \pm 43.6$
Fit Fraction Sum	98.4	100.4					

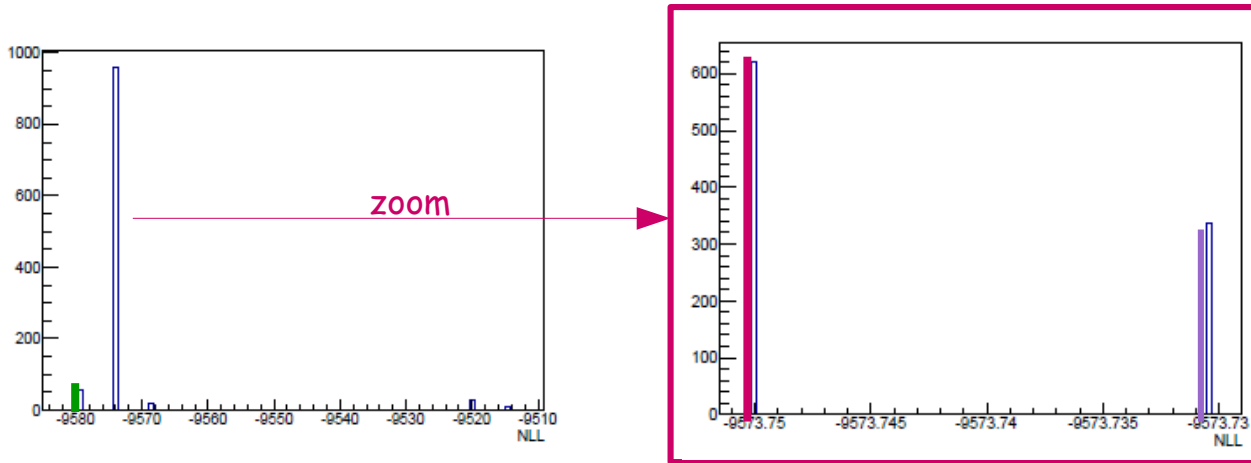


- the model reproduces the data better
- rescattering is responsible for the large CPV, less peaked behavior
- rescattering +  $\rho(1450)$  +  $f_2(1270)$  reproduce the interference pattern @ large  $m_{K\pi}$
- small  $\phi(1020)$

# B → KKπ AmAn: model & fit



- fit stability 2000 randomizing parameter initialization  
interference between  $K^*(1430)$  and  $PolarFormFactor$  produce several nearby solutions

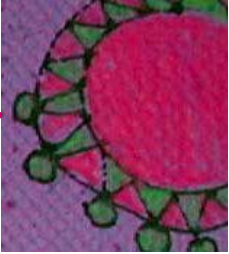


the large interference producing large CPV in  $K^*_0(1430)$  not observed in data is interpreted as a mathematically produced unphysical solution

[NLL -9579]	Fit fraction (%)		Magnitude and phase coefficients				$A_{CP}$ (%)
Component	$B^+$	$B^-$	$a_i^+$	$\delta_i^+ [^\circ]$	$a_i^-$	$\delta_i^- [^\circ]$	
$K^{*0}(892)$	$5.7 \pm 0.8$	$10.4 \pm 1.0$	$0.93 \pm 0.04$	$0 \pm 0$	$1.07 \pm 0.04$	$0 \pm 0$	$14.9 \pm 8.6$
$K^*_0(1430)$	$3.5 \pm 1.2$	$34.9 \pm 3.7$	$0.73 \pm 0.15$	$-176 \pm 10$	$1.97 \pm 0.14$	$-149 \pm 3$	$76.1 \pm 10.2$
$PolarFormFactor$	$30.9 \pm 1.9$	$31.0 \pm 3.0$	$2.16 \pm 0.13$	$-138 \pm 7$	$1.86 \pm 0.13$	$140 \pm 7$	$-15.0 \pm 5.9$

[NLL -9574]	Fit fraction (%)		Magnitude and phase coefficients				$A_{CP}$ (%)
Component	$B^+$	$B^-$	$a_i^+$	$\delta_i^+ [^\circ]$	$a_i^-$	$\delta_i^- [^\circ]$	
$K^{*0}(892)$	$5.7 \pm 0.8$	$9.9 \pm 1.0$	$0.94 \pm 0.04$	$0 \pm 0$	$1.06 \pm 0.04$	$0 \pm 0$	$12.3 \pm 8.7$
$K^*_0(1430)$	$3.5 \pm 0.8$	$5.9 \pm 1.2$	$0.74 \pm 0.09$	$-176 \pm 10$	$0.82 \pm 0.09$	$136 \pm 11$	$10.4 \pm 14.9$
$PolarFormFactor$	$31.0 \pm 2.0$	$34.1 \pm 2.6$	$2.19 \pm 0.13$	$-138 \pm 7$	$1.97 \pm 0.12$	$166 \pm 6$	$-10.7 \pm 5.3$

[NLL -9573]	Fit fraction (%)		Magnitude and phase coefficients				$A_{CP}$ (%)
Component	$B^+$	$B^-$	$a_i^+$	$\delta_i^+ [^\circ]$	$a_i^-$	$\delta_i^- [^\circ]$	
$K^{*0}(892)$	$6.0 \pm 0.8$	$10.4 \pm 1.1$	$0.94 \pm 0.04$	$0 \pm 0$	$1.06 \pm 0.04$	$0 \pm 0$	$12.0 \pm 8.3$
$K^*_0(1430)$	$32.6 \pm 1.7$	$34.9 \pm 2.2$	$2.19 \pm 0.11$	$-85 \pm 7$	$1.94 \pm 0.11$	$-149 \pm 5$	$-11.8 \pm 4.4$
$PolarFormFactor$	$26.9 \pm 2.4$	$31.0 \pm 2.8$	$1.99 \pm 0.13$	$-164 \pm 6$	$1.83 \pm 0.12$	$140 \pm 7$	$-8.2 \pm 6.6$



## ● systematic uncertainties

**1D mass fit** : difference of the parameters ( $\sigma_{\text{sys}} = x - x_{\text{nominal}}$ )

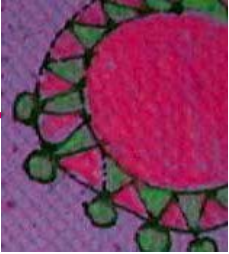
- alternative PDF for the signal model used in the 1D mass fit
- cross-feed background asymmetry:  $\mathcal{A}_{hhh} = \text{Asym} \pm 3 \times \sqrt{\sigma_{\text{stat}}^2 + \sigma_{\text{sys}}^2 + \sigma_{J/\psi}^2}$
- cross-feed background contribution in model.
- different parameters for B+ and B-.
- partially reconstructed decay asymmetry.

**Efficiency description across the Dalitz plot**: spread of the parameter ( $\sigma_{\text{sys}} = \sigma_x$ )

- due the limited statistic of the MC samples (poisson fluctuate).
- PID efficiency error propagation

**Efficiency description across the Dalitz plot**: difference of parameters ( $\sigma_{\text{sys}} = x - x_{\text{nominal}}$ )

- LO trigger efficiency correction, use alternative correction tables.
- binning scheme: finer and coarser binning of the efficiency maps.
- production and detection asymmetry.
- truth match inefficiency



## ● systematic uncertainties (cont)

**Background maps** : spread of the parameter ( $\sigma_{\text{sys}} = \sigma_x$ )

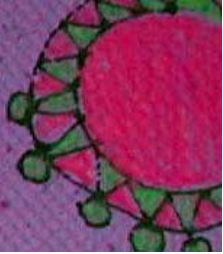
- poisson fluctuate the combinatorial background map.
- poisson fluctuate the cross-feed background map.

## Amplitude Analysis

- fit Bias: generate & fit 1000 Toy MC samples using the baseline model solution ( $\sigma_{\text{sys}} = x - x_{\text{nominal}}$ )
- blatt-weisskopf barrier radii: the Dalitz plot fit is performed considering values for 3-5  $\text{GeV}^{-1}$  ( $\sigma_{\text{sys}} = x - x_{\text{nominal}}$ )
- resonance parameters: mass and width of the resonance components included in the baseline model are randomly varied according to central value and uncertainties are taken from the PDG. ( $\sigma_{\text{sys}} = \sigma_x$ )
- $\rho(1450)$  mass and width: float  $\rho(1450)$  parameters, found to be  $m = 1.55 \pm 0.01 \text{ GeV}$  and  $\Gamma = 0.42 \pm 0.02 \text{ GeV}$  ( $\sigma_{\text{sys}} = x - x_{\text{nominal}}$ )

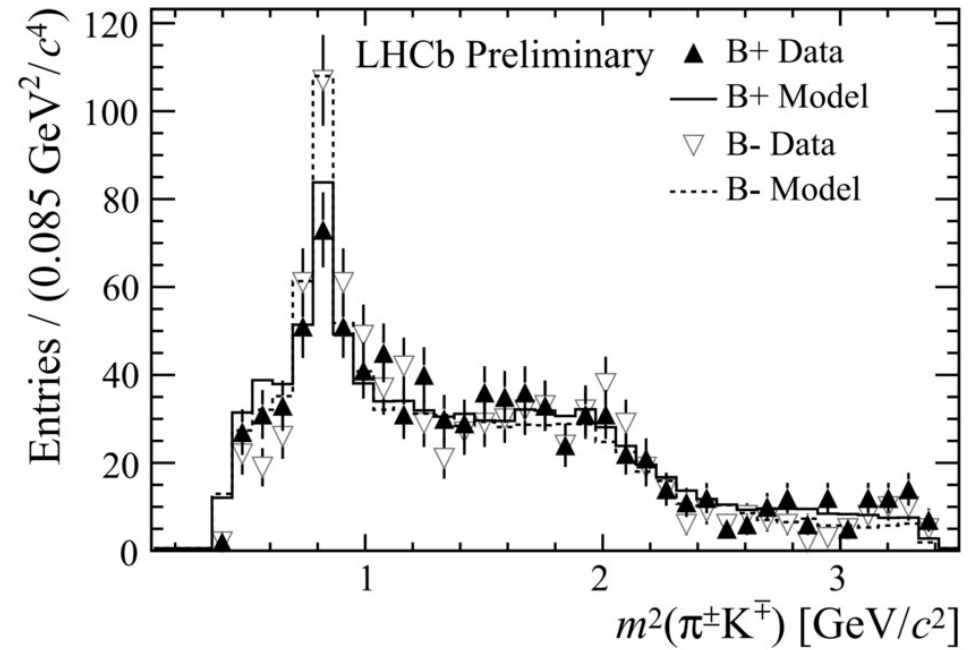
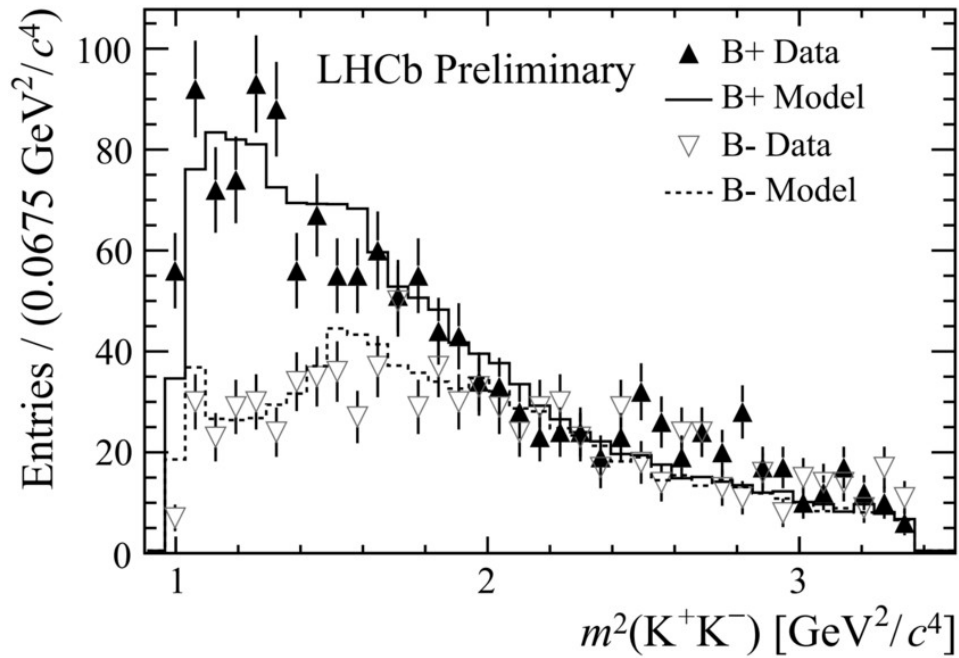
**main sources:** resonance parameters (particularly important for the  $K^*(1430)$  and non-resonant related results)

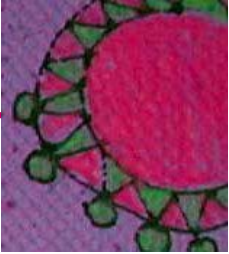
$\rho(1450)$  mass and width



final result including systematic uncertainties

Contribution	Fit Fraction(%)	$A_{CP}$ (%)	Amplitude ( $B^+/B^-$ )	Phase[°] ( $B^+/B^-$ )
$K^*(892)^0$	$7.5 \pm 0.6 \pm 0.5$	$12.3 \pm 8.7 \pm 4.5$	$0.94 \pm 0.04 \pm 0.02$ / $1.06 \pm 0.04 \pm 0.02$	0 (fixed)
$K_0^{*0}(1430)$	$4.5 \pm 0.7 \pm 1.2$	$10.4 \pm 14.9 \pm 8.8$	$0.74 \pm 0.09 \pm 0.09$ / $0.82 \pm 0.09 \pm 0.10$	$-176 \pm 10 \pm 16$ / $136 \pm 11 \pm 21$
Single-Pole Form Factor	$32.3 \pm 1.5 \pm 4.1$	$-10.7 \pm 5.3 \pm 3.5$	$2.19 \pm 0.13 \pm 0.17$ / $1.97 \pm 0.12 \pm 0.20$	$-138 \pm 7 \pm 5$ / $166 \pm 6 \pm 5$
$\rho(1450)$	$30.7 \pm 1.2 \pm 0.9$	$-10.9 \pm 4.4 \pm 2.4$	$2.14 \pm 0.11 \pm 0.07$ / $1.92 \pm 0.10 \pm 0.07$	$-175 \pm 10 \pm 15$ / $140 \pm 13 \pm 20$
$f_2(1270)$	$7.5 \pm 0.8 \pm 0.7$	$26.7 \pm 10.2 \pm 4.8$	$0.86 \pm 0.09 \pm 0.07$ / $1.13 \pm 0.08 \pm 0.05$	$-106 \pm 11 \pm 10$ / $-128 \pm 11 \pm 14$
rescattering	$16.4 \pm 0.8 \pm 1.0$	$-66.4 \pm 3.8 \pm 1.9$	$1.91 \pm 0.09 \pm 0.06$ / $0.86 \pm 0.07 \pm 0.04$	$-56 \pm 12 \pm 18$ / $-81 \pm 14 \pm 15$
$\phi(1020)$	$0.3 \pm 0.1 \pm 0.09$	$9.8 \pm 43.6 \pm 26.6$	$0.20 \pm 0.07 \pm 0.02$ / $0.22 \pm 0.06 \pm 0.04$	$-52 \pm 23 \pm 32$ / $107 \pm 33 \pm 41$





- The model represent the data well and the inclusion of run2 data is very important.

LHCb RUN1+ RUN2 ~30K events

- rescattering hypothesis is able to describe the large CPV observed

- rescattering must be polished

arXiv:1807.04543v1 [hep-ph] 12 Jul 2018

$\pi\pi \rightarrow K\bar{K}$  scattering up to 1.47 GeV with hyperbolic dispersion relations

J.R. Pelaez, A. Rodas (U. Complutense de Madrid)

- interference structure at large  $m_{K\pi}$  involve the scalar and the vector

- measure the KK vector mass of  $1.55 \pm 0.01$  GeV and width of  $0.42 \pm 0.02$  GeV

$\rho(1450)$  [r]

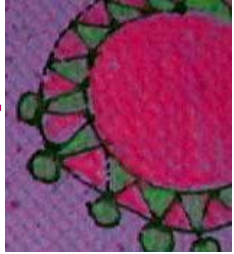
Mass  $m = 1465 \pm 25$  MeV [l]  
Full width  $\Gamma = 400 \pm 60$  MeV [l]

$\phi(1680)$

Mass  $m = 1680 \pm 20$  MeV [l]  
Full width  $\Gamma = 150 \pm 50$  MeV [l]

- the fit requires a  $f_2(1270)$  and not a  $f'_2(1525)$

- broad scalars are always troublesome



## $\pi\pi \rightarrow K\bar{K}$ scattering up to 1.47 GeV with hyperbolic dispersion relations.

J.R. Pelaez<sup>1</sup> and A.Rodas<sup>1</sup>

<sup>1</sup>*Departamento de Física Teórica, Universidad Complutense de Madrid, 28040 Madrid, Spain*

In this work we provide a dispersive analysis of  $\pi\pi \rightarrow K\bar{K}$  scattering. For this purpose we present a set of partial-wave hyperbolic dispersion relations using a family of hyperbolas that maximizes the applicability range of the hyperbolic dispersive representation, which we have extended up to 1.47 GeV. We then use these equations first to test simple fits to different and often conflicting data sets, also showing that some of these data and some popular parameterizations of these waves fail to satisfy the dispersive analysis. Our main result is obtained after imposing these new relations as constraints on the data fits. We thus provide simple and precise parameterizations for the S, P and D waves that describe the experimental data from  $K\bar{K}$  threshold up to 2 GeV, while being consistent with crossing symmetric partial-wave dispersion relations up to their maximum applicability range of 1.47 GeV. For the S-wave we have found that two solutions describing two conflicting data sets are possible. The dispersion relations also provide a representation for S, P and D waves in the pseudo-physical region.

arXiv:1807.04543v2 [hep-ph] 2 Nov 2018

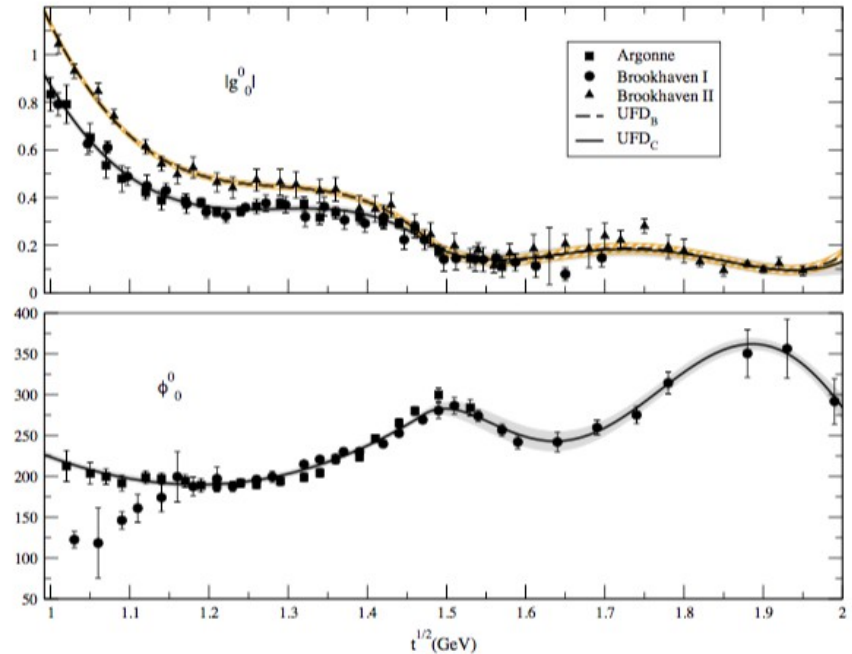


FIG. 4: Upper panel: Modulus of the scalar-isoscalar  $\pi\pi \rightarrow K\bar{K}$  scattering. The continuous line represents the  $\text{UFD}_C$  parameterization while the dashed line represents the  $\text{UFD}_B$  fit to the Brookhaven-II data only. Lower panel: Scalar-isoscalar  $\text{UFD}$  phase for  $\pi\pi \rightarrow K\bar{K}$  scattering, which is common for both  $\text{UFD}_B$  and  $\text{UFD}_C$ . Note that the Brookhaven-I phase close to threshold lies around  $150^\circ$  or below, at odds with all dispersive analysis of  $\pi\pi$  scattering, which find a phase around or above  $200^\circ$ .